

<b>REPORT DOCUMENTATION PAGE</b>				<i>Form Approved</i> OMB No. 0704-0188	
<p>The public reporting burden for this collection of information is estimated to average 1 hour per response, including the time for reviewing instructions, searching existing data sources, gathering and maintaining the data needed, and completing and reviewing the collection of information. Send comments regarding this burden estimate or any other aspect of this collection of information, including suggestions for reducing the burden, to Department of Defense, Washington Headquarters Services, Directorate for Information Operations and Reports (0704-0188), 1215 Jefferson Davis Highway, Suite 1204, Arlington, VA 22202-4302. Respondents should be aware that notwithstanding any other provision of law, no person shall be subject to any penalty for failing to comply with a collection of information if it does not display a currently valid OMB control number.</p> <p><b>PLEASE DO NOT RETURN YOUR FORM TO THE ABOVE ADDRESS.</b></p>					
<b>1. REPORT DATE (DD-MM-YYYY)</b> 14-01-2015		<b>2. REPORT TYPE</b> Final		<b>3. DATES COVERED (From - To)</b> 24 Jun 2013 – 24 Sep 2014	
<b>4. TITLE AND SUBTITLE</b>  Practical Method to Identify Orbital Anomaly as Breakup Event in the Geostationary Region				<b>5a. CONTRACT NUMBER</b> FA23861314076	
				<b>5b. GRANT NUMBER</b> Grant AOARD-134076	
				<b>5c. PROGRAM ELEMENT NUMBER</b> 61102F	
<b>6. AUTHOR(S)</b>  Dr Yukihiro Kitazawa				<b>5d. PROJECT NUMBER</b>	
				<b>5e. TASK NUMBER</b>	
				<b>5f. WORK UNIT NUMBER</b>	
<b>7. PERFORMING ORGANIZATION NAME(S) AND ADDRESS(ES)</b> IHI Corporation 1-1, Toyosu 3-chome, Koto-ku Tokyo Japan				<b>8. PERFORMING ORGANIZATION REPORT NUMBER</b>  N/A	
<b>9. SPONSORING/MONITORING AGENCY NAME(S) AND ADDRESS(ES)</b>  AOARD UNIT 45002 APO AP 96338-5002				<b>10. SPONSOR/MONITOR'S ACRONYM(S)</b>  AFRL/AFOSR/IOA(AOARD)	
				<b>11. SPONSOR/MONITOR'S REPORT NUMBER(S)</b>  AOARD-134076	
<b>12. DISTRIBUTION/AVAILABILITY STATEMENT</b> Distribution A:Approved for public release. Distribution is unlimited.					
<b>13. SUPPLEMENTARY NOTES</b>					
<b>14. ABSTRACT</b> Orbital anomalies observed in the geostationary region are suspected to originate in breakup. This granted study aims to identify these orbital anomalies as breakup events by actual ground-based optical surveys and origin identifications of uncorrelated targets. Previous work proposed an effective search strategy applicable for breakup fragments in the geostationary region by predicting the population and the motion of fragmentation debris. This paper details the strategy and reports the actual observation applications. The observation was performed at Bisei Spaceguard Center, Okayama, Japan. Two breakup events are selected as targets for observation campaigns. Both are US Titan 3C Transtages. As a result of the observation of 1968-081E, thirty-one uncorrelated targets were detected and the orbits of seven objects were successfully determined. The origin identification of the seven objects was conducted with the determined orbits, and one object is correlated with 1968-081E. Moreover, two objects are associated with unconfirmed breakups of the US Titan 3C Transtages of 1973-040B and 1975-118C. The orbits of the two uncorrelated objects and the motions well matched with the predicted populations and motions of the parent objects. As a result of the observation of 1967-066G, five uncorrelated objects were detected, and the orbits of two objects were well estimated. However, both objects are not associated with the target or the other candidates.					
<b>15. SUBJECT TERMS</b> Space Debris, Space Technology, orbit determination					
<b>16. SECURITY CLASSIFICATION OF:</b>			<b>17. LIMITATION OF ABSTRACT</b>	<b>18. NUMBER OF PAGES</b>	<b>19a. NAME OF RESPONSIBLE PERSON</b> Ingrid J. Wysong, Ph.D.
<b>a. REPORT</b>	<b>b. ABSTRACT</b>	<b>c. THIS PAGE</b>			
U	U	U	SAR	24	+81-3-5410-4409

# **Final Performance Report**

## **Practical Method to Identify Orbital Anomaly as Breakup Event in the Geostationary Region (AOARD 134076)**

**Yukihito Kitazawa<sup>\*</sup>**

<sup>\*</sup>IHI Corporation, Toyosu IHI Building 1-1, Toyosu 3-chome, Koto-ku, Tokyo 135-8710,  
Japan



## ABSTRACT

Orbital anomalies observed in the geostationary region are suspected to originate in breakups. This granted study aims to identify these orbital anomalies as breakup events by actual ground-based optical surveys and origin identifications of uncorrelated targets. The past granted study proposed an effective search strategy applicable for breakup fragments in the geostationary region. This strategy predicts the population and the motion of fragmentation debris from a specific breakup event by using orbital debris modeling techniques. This paper explains the proposed strategy and reports the actual observations applying the strategy. The observations were performed at Bisei Spaceguard Center, Okayama prefecture, Japan. Two breakup events are selected as targets for observation campaigns. Both are US Titan 3C Transtages. One is 1968-081E exploded in February 1992, and the other is 1967-066G experienced an abrupt orbital change in February 1994. As a result of the observation of 1968-081E, thirty-one uncorrelated targets were detected and the orbits of seven objects were successfully determined. The origin identification of the seven objects was conducted with the determined orbits, and one object is associated with 1968-081E. Moreover, two objects are associated with unconfirmed breakups of the US Titan 3C Transtages of 1973-040B and 1975-118C. The orbits of the two uncorrelated objects and the motions well matched with the predicted populations and motions of the parent objects. As a result of the observations targeting 1967-066G, five uncorrelated objects were detected, and the orbits of two objects were well estimated. However, both objects are not associated with the target or the other candidates.

## 1. INTRODUCTION

On 4<sup>th</sup> June 2014, the breakup of an old rocket body, the US Titan 3C Transtage (International Designator: 1969-013B) was observed in the geostationary region (here defined as orbits with mean motion between 0.9 and 1.1 revolutions per day, eccentricity smaller than 0.2 and inclination below 30 degrees) (Ref. [1]). In addition to this breakup, two breakups have been confirmed in this region (Ref. [2]). One is the Russian Ekran 2 (International Designator: 1977-092A) breakup on 23<sup>rd</sup> June 1978. This was the first known fragmentation in the geostationary region. Another is the US Titan IIIC Transtage (International Designator: 1968-081E) breakup on 21<sup>st</sup> February 1992. Moreover, European Space Agency (ESA) has concluded that ten additional events listed in Table 1 should be taken into account to describe the present space debris environment in the geostationary region (Ref. [3-5]). Observations performed by ESA using larger aperture telescopes detected enormous number of uncorrelated debris and indicate that these objects may have originated from these energetic explosions. In addition, some scientists have found evidence for historical satellite fragmentations in the geostationary region (Ref. [6-8]).

Table 1. The breakup objects in the GEO region

International Designator	Object name [object type]	Breakup epoch [yyddd.dddd]
1977-092A	Ekran 2 [spacecraft]	78174.0000
1973-040B	US Titan3C Transtage [rocket body]	81067.2007
1979-087A	Ekran 4 [spacecraft]	82157.7550
1979-053C	US Titan3C Transtage [rocket body]	82309.0000
1975-118C	US Titan3C Transtage [rocket body]	87072.6430
1966-053J	US Titan3C Transtage [rocket body]	87276.6882
1968-081E	US Titan3C Transtage [rocket body]	92053.3745
1967-066G	US Titan3C Transtage [rocket body]	94045.4161
1975-117A	SATCOM 1 [spacecraft]	99257.6799
1988-018B	TELECOM 1C [spacecraft]	02263.0000
1969-013B	US Titan3C Transtage [rocket body]	14155.1097
AE-02	[N/A]	98180.0000
AE-03	[N/A]	92280.0000

It has been revealed in [6] that four very old Titan IIIC Transtages (1966-053J, 1967-066G, 1973-100D, 1978-113D) have experienced abrupt orbital changes for unknown reasons. It also has been revealed in [6] that no debris clouds have been yet associated with these Transtages. On the other hand, six old Titan IIIC Transtages (1966-053J, 1967-066G, 1968-081E, 1973-040B, 1975-118C, 1979-053C) have been listed in [5] as those have released fragments, including a known breakup event of 1968-081E. To describe the present space debris environment in the geostationary region the ESA MASTER-2009 includes the six Transtages listed in [5] as those have released fragments.

The three Transtages of 1973-040B, 1975-118C, and 1979-053C have not been listed in [6] as those have experienced abrupt orbital changes, even though these Transtages have been listed in [5] as those have released fragments. In contrary, the two Transtages of 1973-100D and 1978-113D have not been listed in [5] as those have released fragments, even though these Transtages have been listed in [6] as those have experienced abrupt orbital changes. Therefore, this granted study aims to confirm which of Transtages have actually released fragments.

This granted study has proposed an effective search and origin identification strategy applicable for the optical survey of breakup debris. In the proposed strategy, the population and the motion of the fragmentation debris generated from a specific breakup event can be predicted by orbital debris modeling techniques. The orbital debris modeling techniques describe debris generation and orbit propagation. The NASA standard breakup model [9] is used for debris generation, whereas the orbit propagation is based on an original orbit propagator developed for this granted study [10].

First, this granted study performed the search observation of uncorrelated objects from a confirmed breakup event and origin identification of detected objects. The observation was conducted by 1-m aperture telescope at Bisei Spaceguard Center (BSGC), Okayama Prefecture, Japan. BSGC adopts the Time Delay Integration (TDI) method as the imaging method of the Charge Coupled Device (CCD) sensor. We applied the proposed search strategy to the TDI method and build the observation planning customized to BSGC (see Appendix A). The target of this observation was the US Titan 3C Transtage of 1968-081E. The observation campaign was performed for two months. As the result of this observation, thirty-one uncorrelated objects were detected and the orbits of seven objects were determined. We also conducted the origin identifications of the seven objects by using the orbits, and one object was associated with 1968-081E. Moreover, two objects were correlated with other unconfirmed breakups 1973-040B and 1975-118C, which these objects are listed in [5] as the suspicious fragmentations. Therefore, the usefulness of the proposed debris modeling techniques was validated.

Second, this granted study conducted the search observation of uncorrelated fragments released from the unconfirmed breakup 1967-066G, that the abrupt orbital change was observed on February 1994. As the result of this observation, five uncorrelated objects were detected, and the orbits of two objects were successfully determined. However, no objects were associated with the target breakup event. Note that this object was also selected as the observation target in the past granted study, but any uncorrelated objects were not associated with the target.

## 2. STRATEGY OVERVIEW

### 2.1. Orbital debris modeling techniques

The orbital debris modeling techniques describe the debris generation and the orbital propagation. The population and the motion of the target fragments at an observation epoch can be predicted by the techniques. The physical properties of the fragmentation debris generated by a breakup are given by the debris generation, whereas the behavior of the space object is described by the orbit propagation. Therefore, the population and the motion can be predicted as mentioned in [11]. The NASA Standard Breakup Model [9] and an original orbital propagator developed for this granted study [10] are used for the debris generation and the orbit propagation, respectively. The observation point is determined based on the population prediction. Figure 1 demonstrates the population prediction of 1968-081E fragments on 3<sup>rd</sup> March 2014. Two peaks can be seen at Point A (358.5, 4.5) [deg.] and Point B (178.5, -4.5) [deg.] in Figure 1. One can specify an observation point by estimating the elevations of each point. Figure 2 represents the predicted motion of the fragments at Point B, which the observatory and the tracking mode of the telescope were defined as BSGC and the sidereal tracking, respectively. In this case, the most likely motion is (-15.3, 1.8) [arc-sec/sec].

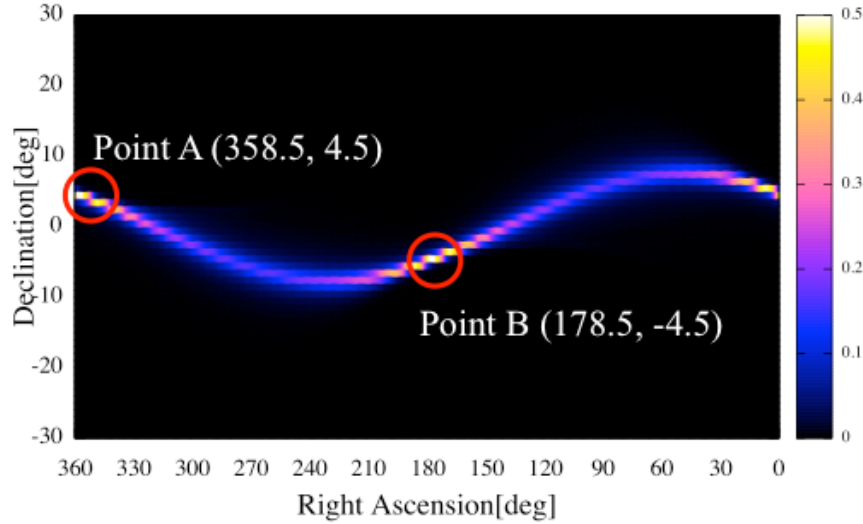


Figure 1. Predicted population of 1968-081E fragments on 3<sup>rd</sup> March 2014

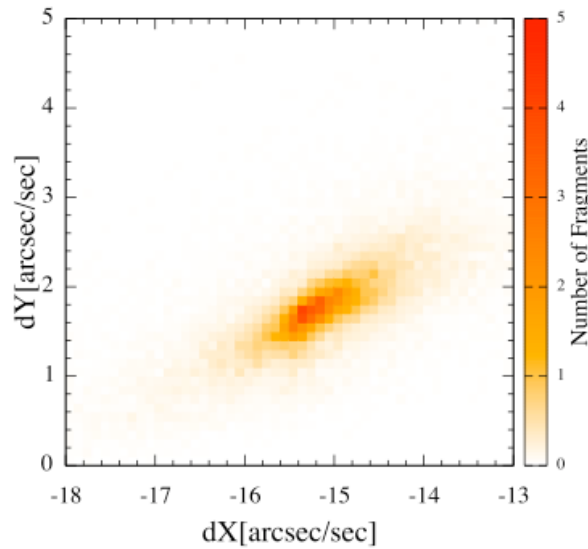


Figure 2. Predicted motion of 1968-081E fragments at Point B (Observatory: BSGC, Tracking mode: sidereal tracking)

## 2.2. Effective search strategy for breakup fragments

Figure 3 represents the effective search and origin identification strategy applicable for breakup fragments. This strategy consists of three steps, “Planning”, “Observation”, and “Verification”. In the first step “Planning”, the target breakup event is selected from thirteen parent objects listed in Table 1, and the fragmentation debris from the target breakup are characterized for the survey observation by the orbital debris modeling techniques. The orbital debris modeling techniques predict the population and the motion of the target breakup fragments, and when, where, and how one should survey is provided as an observation plan. In the second step “Observation”, the survey observation is performed based on the observation plan. The high accuracy orbit needs to be acquired in this step for the long-term propagation from the detection epoch to the breakup epoch in the next step “Verification”. Finally, the origin of the uncorrelated object is identified in the third step “Verification”. The orbit is propagated backward until the date and time each breakup is supposed to take place, and the features of the orbit are compared with each other. The motion of the object obtained in the survey observation is also available for the origin identification by being compared with the predicted motion. The origin of the detected object can be referred for verification of unconfirmed breakup events and the next target determination.

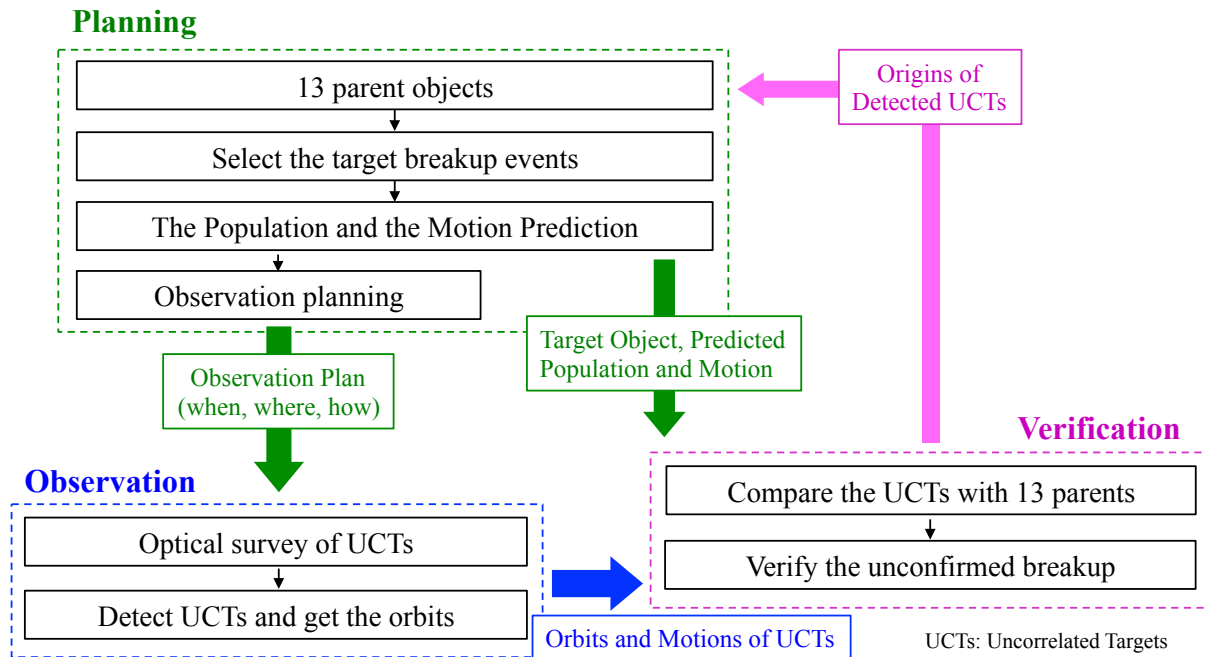


Figure 3. The effective search and origin identification strategy applicable for the breakup fragments

### 3. THE OBSERVATION CAMPAIGN OF 1968-081E FRAGMENTS

#### 3.1. Observation overview

In the past granted study, the search observation of uncorrelated objects was conducted at JAXA Nyukasa Observatory (JNO), Nagano Prefecture, Japan, whereas this granted study performed the observation at Bisei Spaceguard Center (BSGC). BSGC adopts the Time Delay Integration (TDI) method as the imaging method of the Charge Coupled Device (CCD) sensor. We applied the proposed strategy to the TDI method in this observation (see Appendix A). The target breakup event of this observation was the US Titan 3C Transtage of 1968-081E. Table 2 summarizes the overview of this observation including the technical information of the observatory. One-month observation campaign had been performed twice, and an observation plan had been built once a week. Note that the survey observations had actually conducted for sixteen nights because of the condition of the weather, the age of the moon, or the schedule of the follow-up observations. The aperture of the telescope was 1m. The total sky coverage of the image area of the system was around 1.21 degrees by 2.47 degrees, and its pixel scale was 1.06 arc seconds.

Table 2. The overview of the observation at BSGC [12]

Target breakup event	US Titan 3C Transtage (International Designator: 1968-081E)
Observation period	10 <sup>th</sup> November 2013 – 30 <sup>th</sup> November 2013 (survey: 7 nights) 20 <sup>th</sup> February 2014 – 20 <sup>th</sup> March 2014 (survey: 9 nights)
Observatory	Bisei Spaceguard Center, Okayama prefecture, Japan (133.32°40" E, 34.40°21" N, 463 m altitude)
Telescope	aperture: 1-m, final focal ratio: f/3, set on a fork-type equatorial mount
CCD sensor	four 2k by 4k fully-depleted back illuminated CCDs, total field-of-view: 1.2 by 2.5 [deg], 1.06 [arc-sec/pixel]

Table 3 informs the result of the survey observations. As the result of the sixteen nights survey observations, thirty-one uncorrelated objects were detected. Moreover, the orbits of seven objects were successfully determined by the follow-up observations, which were described in red in Table 3.

Table 3. The results of the survey observations

Date [yyymmdd]	Observation point			Detected object label
	R.A. [deg]	Dec. [deg]	Radius [km]	
131110	358.5	4.5	41900.0	x15264
131111	358.5	4.5	41900.0	x15267, x15268
131112	358.5	4.5	41900.0	-
131113	358.5	4.5	41900.0	-
131125	357.5	4.5	41900.0	-
131126	357.5	4.5	41900.0	x15292, x15293, x15294, x15295
131128	357.5	4.5	41900.0	x15298, x15299, x15300
140220	177.5	-5.5	41700.0	x15403
140221	177.5	-5.5	41700.0	x15406, x15407
140223	177.5	-5.5	41700.0	x15411, x15412, x15413, x15414, x15415, x15416, x15417, x15418
140224	177.5	-5.5	41700.0	x15419
140303	178.5	-5.5	41700.0	x15423, x15424, x15425, x15426, x15427
140306	178.5	-5.5	41700.0	x15429, x15430
140307	178.5	-5.5	41700.0	-
140310	178.5	-5.5	41700.0	x15437, x15438
140311	178.5	-5.5	41700.0	-

### 3.2. Origin identification

The origin identifications of the seven objects were conducted with the determined orbits. In this analysis, the orbits of the seven objects were propagated backward until the breakup epochs of the all candidates listed in Table 1 except 1969-013B and compared with each parent in terms of the following points:

- Inclination vectors ( $i \times \cos(\Omega)$ ,  $i \times \sin(\Omega)$ )
- Pinch point
- Geocentric distance at the pinch point

Table 4 summarizes the results of the origin identifications. One object labeled x15300 was correlated with the target 1968-081E. Figures 4 – 6 represent the results of each analysis of x15300. The features of the orbit of x15300 well matched with the 1968-081E. In addition to that, two objects labeled x15429 and x15430 were associated with 1974-040B and 1979-118C, respectively. Figures 7 – 9 and Figures 10 – 12 represent the result. Both breakup events are listed in [5] as the unconfirmed breakups of US Titan 3C Transtages.

Table 4. The result of origin identification of the seven detected objects

Object name	Parent object	Inclination vector	Pinch point	Geocentric distance
x15264	1967-066G	Fair	Good	Poor
x15267	-	-	-	-
x15300	1968-081E	Good	Good	Good
x15426	1967-066G	Fair	Good	Poor
x15429	1973-040B	Good	Good	Good
x15430	1975-118C	Good	Good	Good
	1973-040B	Fair	Good	Fair
x15438	1977-092A	Good	Good	Poor
	1975-118C	Fair	Good	Fair
	1968-081E	Fair	Good	Fair

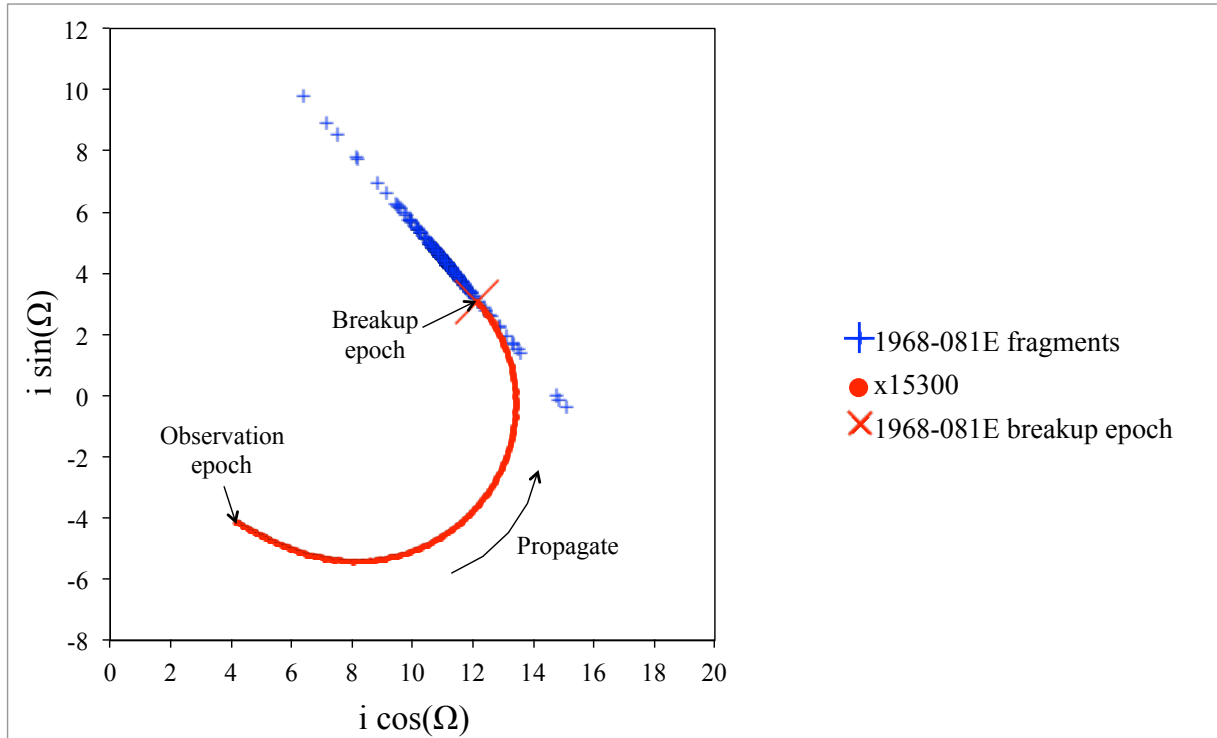


Figure 4. The inclination vectors ( $i \cos \Omega$ ,  $i \sin \Omega$ ) of 1968-081E and x15300 at the breakup epoch of 1968-081E

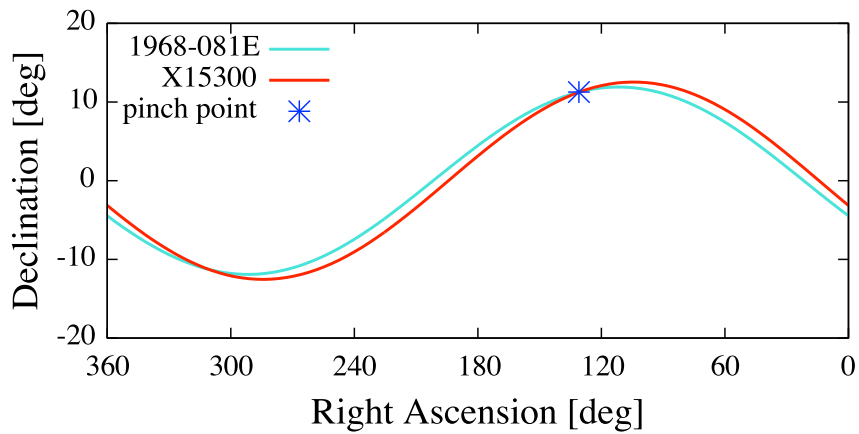


Figure 5. The pinch point of 1968-081E and the intersection of the orbits of 1968-081E and x15300

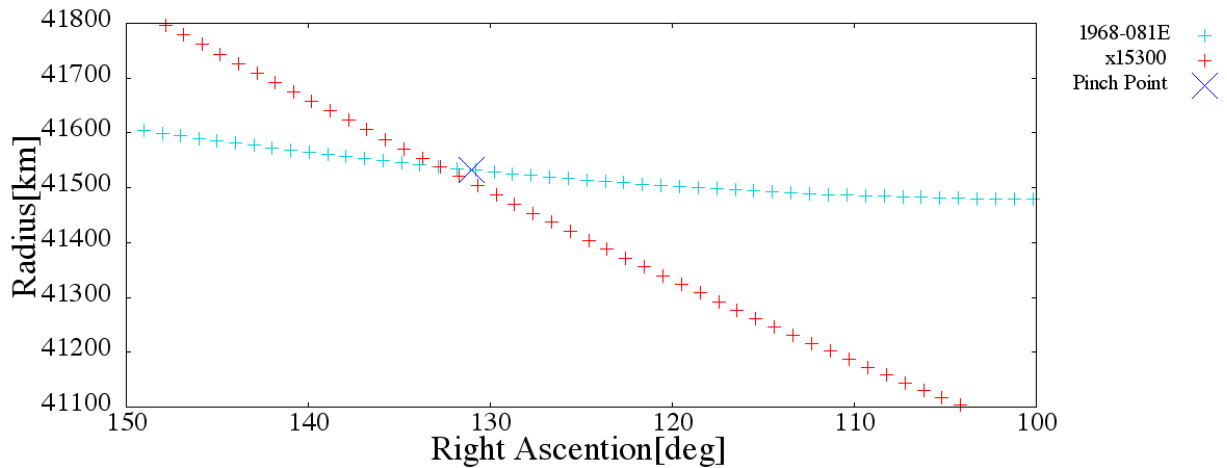


Figure 6. The radii of 1968-081E and x15300 at the pinch point

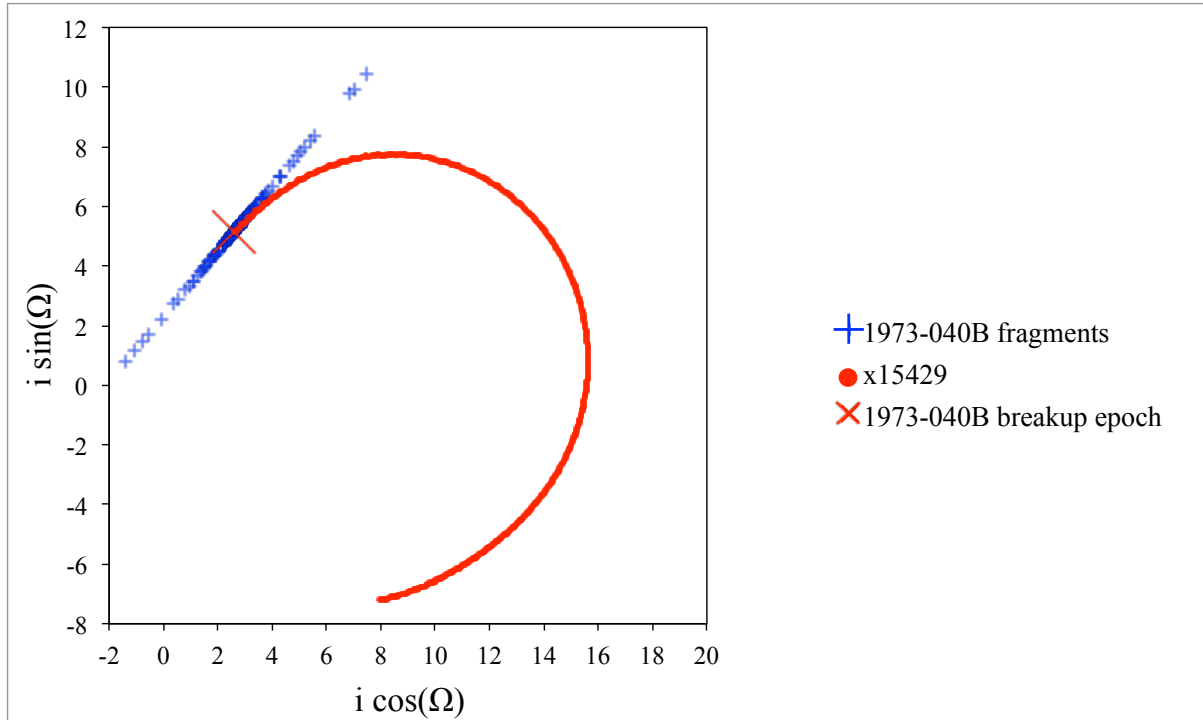


Figure 7. The inclination vectors ( $i \cos \Omega$ ,  $i \sin \Omega$ ) of 1973-040B and x15429 at the breakup epoch of 1973-040B

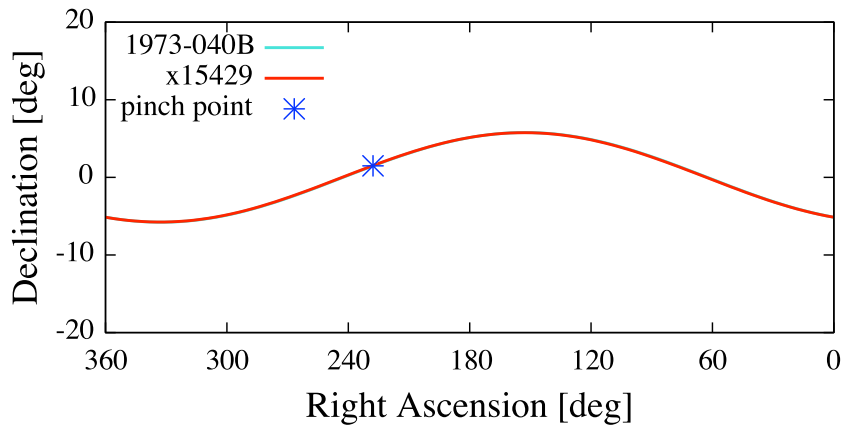


Figure 8. The pinch point of 1973-040B and the intersection of the orbits of 1973-040B and x15429

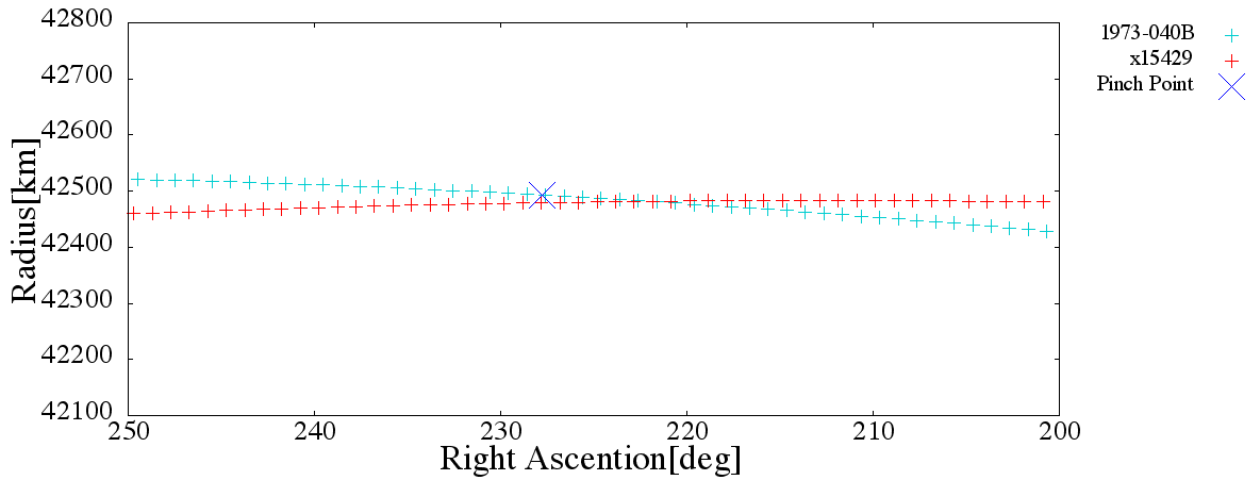


Figure 9. The radii of 1973-040B and x15429 at the pinch point

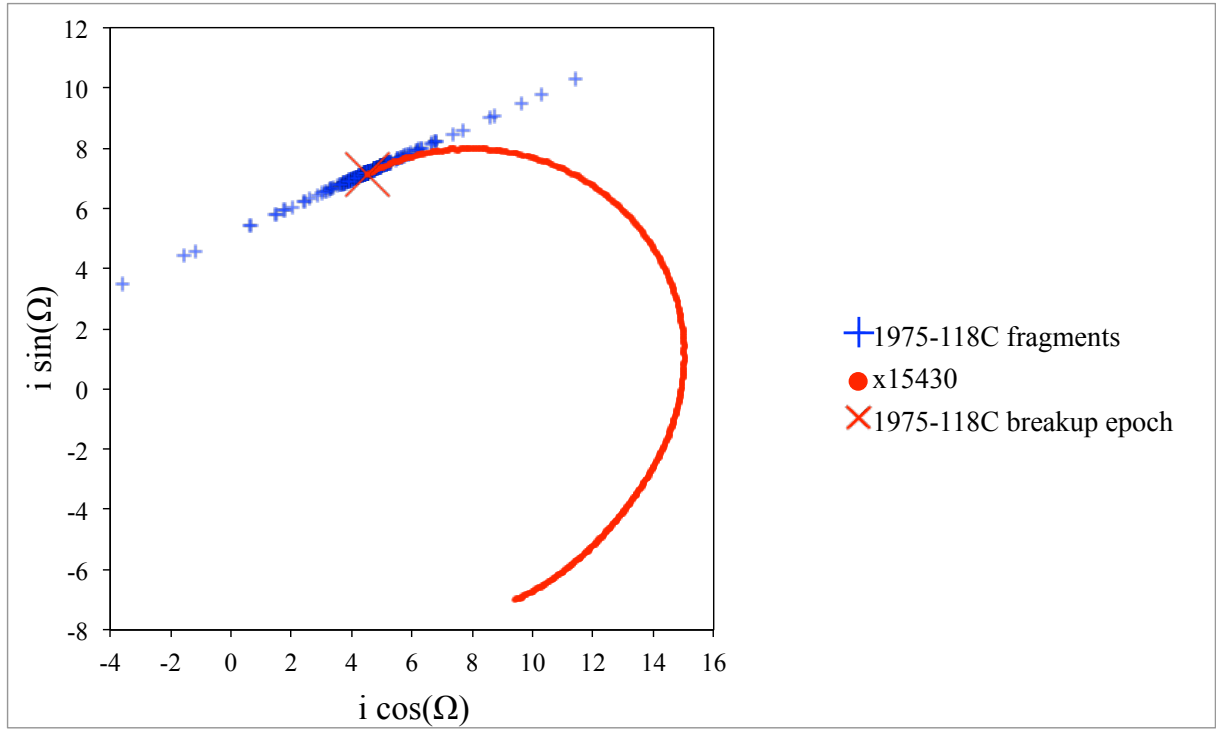


Figure 10. The inclination vectors ( $i \cos \Omega$ ,  $i \sin \Omega$ ) of 1975-118C and x15430 at the breakup epoch of 1975-118C

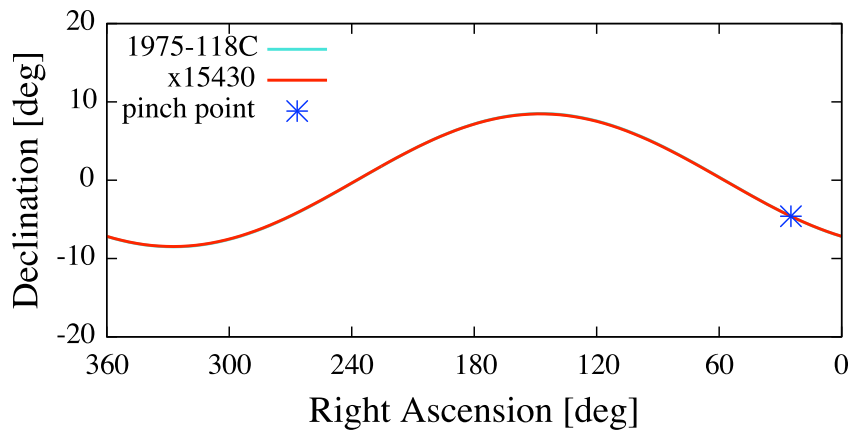


Figure 11. The pinch point of 1975-118C and the intersection of the orbits of 1968-081E and x15430

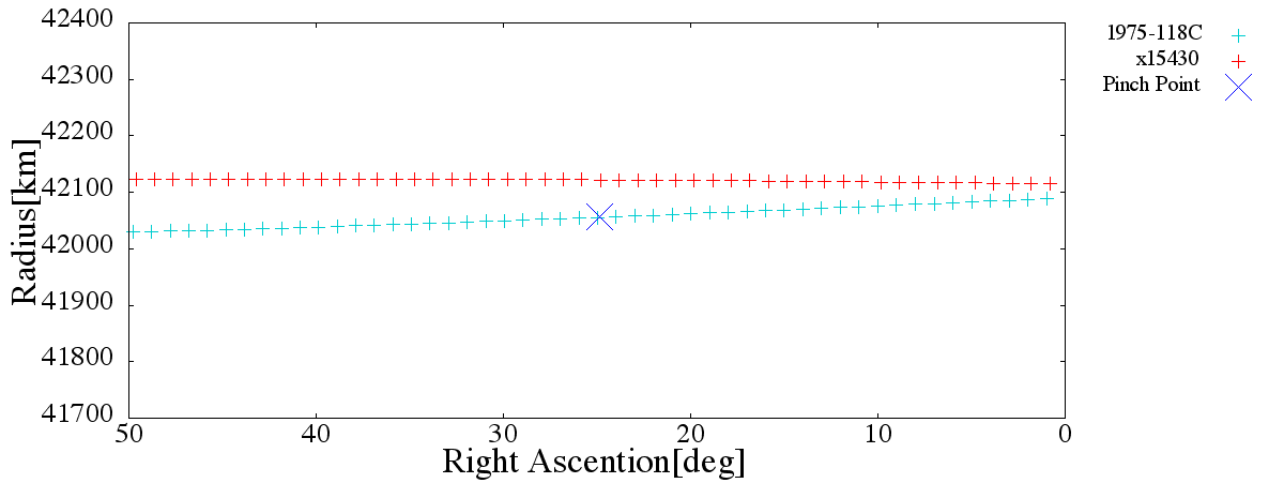


Figure 12. The radii of 1975-118C and x15430 at the pinch point

### 3.3. Population and motion analysis of x15300, x15429, and x15430

Figures 13-15 are the comparisons between the predictions and the measured values of x15300, x15429, and x15430. The trajectories in red and the asterisks in blue represent the orbits and the motions of these objects, respectively. The orbit of x15300 goes through the high possibility region of the predicted population, and the orbits of x15429 and x15430 well matched with the predictions. Also, the motion of x15429 and x15430 matched with each parent objects. The motion of x15300 was a little far from the most likely motion. As demonstrated in Appendix C, the feature of the motion does not always match with the predicted motion even if the features of the orbit well match with the parent object. We can conclude that the proposed strategy works well in the case of the survey of the uncorrelated fragments generated by unconfirmed breakup.

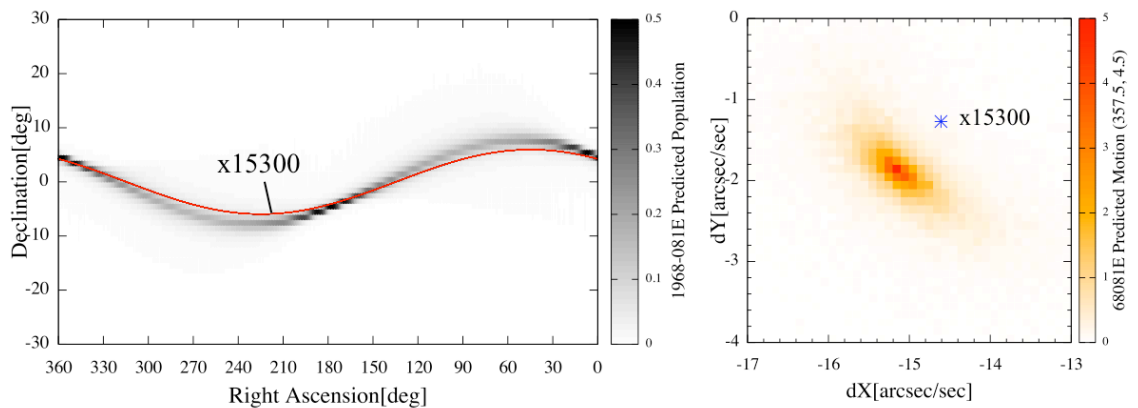


Figure 13. Predicted population of 1968-081E fragments and the orbit of x15300 (left), the predicted motion and the measured motion (right)

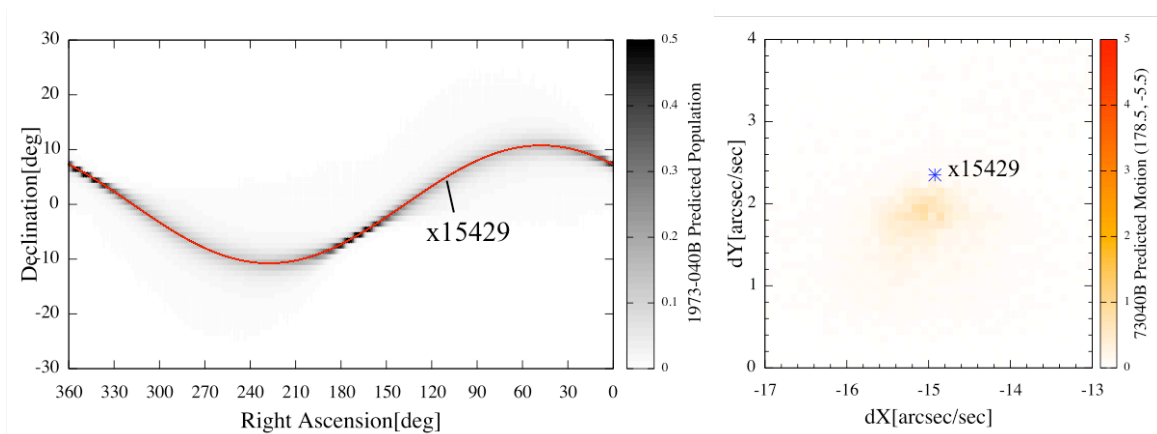


Figure 14. Predicted population of 1973-040B fragments and the orbit of x15429 (left), the predicted motion and the measured motion (right)

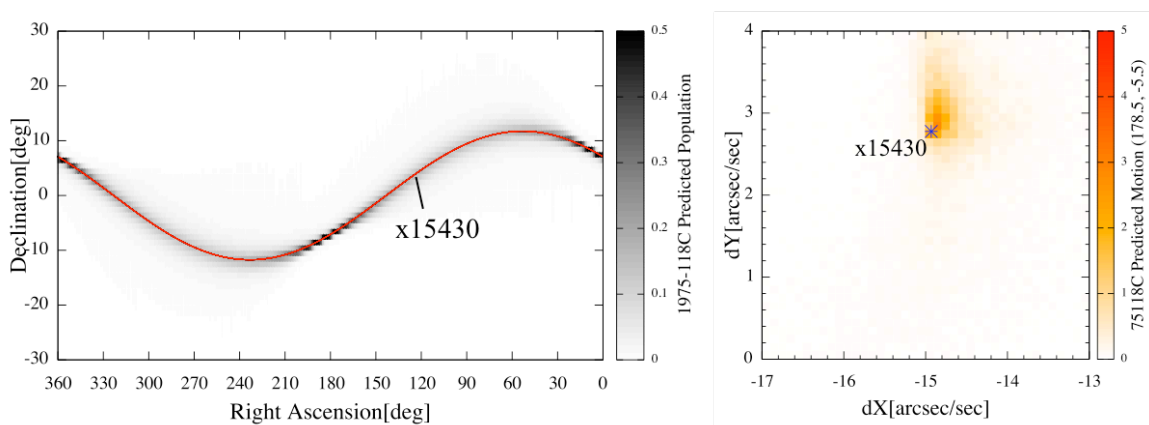


Figure 15. Predicted population of 1975-118C fragments and the orbit of x15430 (left), the predicted motion and the measured motion (right)

#### 4. THE OBSERVATION CAMPAIGN OF 1967-066G FRAGMENTS

This granted study also conducted the survey of the uncorrelated objects generated by the unconfirmed breakup of the US Titan 3C Transtage of 1967-066G. The past granted study also performed the survey of unknown fragments from this event at JNO. However, any uncorrelated objects were not associated with the event. Table 5 informs the overview of this observation. The observatory and the equipment were same with the observation of the 1968-081E fragments. Table 6 summarizes the result of this observation campaign. The survey observations were performed for four nights, and five unknown objects were detected. Moreover, the orbits of two objects were successfully determined by the follow-up observations, which described in red in Table 6.

Table 5. The overview of the observation at BSGC

Target breakup event	US Titan 3C Transtage (International Designator: 1967-066G)
Observation period	20 <sup>th</sup> April 2014 – 26 <sup>th</sup> April 2014 (survey: 2 nights) 25 <sup>th</sup> May 2014 – 3 <sup>rd</sup> June 2014 (survey: 1 night)
Observatory	Bisei Spaceguard Center, Okayama prefecture, Japan (133.32'40" E, 34.40'21" N, 463 m altitude)
Telescope	aperture: 1-m, final focal ratio: f/3, set on a fork-type equatorial mount
CCD sensor	four 2k by 4k fully-depleted back illuminated CCDs, total field-of-view: 1.2 by 2.5 [deg], 1.06 [arcseconds/pixel]

Table 6. The result of the four nights survey observations

Date [yymmdd]	Observation point			Detected object name
	R.A. [deg]	Dec. [deg]	Radius [km]	
140422	169.5	-5.5	40000.0	-
140423	169.5	-5.5	40000.0	x15496, x15497, x15498, x15499
140424	169.5	-5.5	40000.0	-
140529	195.5	-7.5	40000.0	x15534

As the observation of 1968-081E fragments, the origin identification of x15499 and x15534 were performed. However, both objects were not associated with any candidates listed in Table 1. The effectiveness of the proposed strategy for the survey of the uncorrelated fragments generated by unconfirmed breakup was verified in the 1968-081E observation campaign. In addition, taking the results of the observation of the past granted study, we concluded about the orbital anomaly of 1967-066G as follows:

1. There is little possibility to experience a catastrophic explosion.
2. This breakup was quite small so as to release few fragments.
3. The orbital anomaly may be caused by fuel discharge not to release any fragments.

#### 5. CONCLUSIONS

This granted study applied the proposed strategy to the survey of fragmentation debris from unconfirmed breakups and successfully discovered the uncorrelated targets, being associated with the unconfirmed breakups of the US Titan 3C Transtages of 1973-040B and 1975-118C. This outcome has validated our search strategy for unconfirmed breakup fragments and is an evidence of these unconfirmed breakups. On the other hand, it is concluded that 1967-066G may not fragment totally.

As discussed in Appendix B, revisiting the observation for the previous granted study has revealed that one object is associated with the unconfirmed breakup of Russian Ekran 4. Besides the survey of the Transtages, the other breakup objects also need to be researched to elucidate the debris environment in the geostationary region.

#### REFERENCES

1. NASA Orbital Debris Program Office, Orbital Debris Quarterly News, Volume 18, Issue 1, 2014.
2. Johnson, N. L., Stansbery, E., Whitlock, D. O., Abercromby, K. J., Shoots, D., "History of On-orbit Satellite Fragmentations 14th Edition," NASA TM-2008-214779, Jun. 2008.
3. Krag, H., "PROOF-2001," Minutes of the 20th Inter-Agency Space Debris Coordination Committee

- Meeting, Guildford, England, U.K., Apr. 2002.
4. Krag, H., "Status of MASTER-2001 Development," Minutes of the 20th Inter-Agency Space Debris Coordination Committee Meeting, Guildford, England, U.K., Apr. 2002.
  5. Oswald, M., "New Contributions to Space Debris Environment Modeling," Shaker Verlag GmbH, Germany, 2008.
  6. Johnson, N. L., "Evidence for Historical Satellite Fragmentations in and Near the Geosynchronous Regime," Proceedings of the Third European Conference on Space Debris, ESA SP-473, Darmstadt, Germany, 2001, pp.355–359.
  7. Rykhlova, L. V., Kasimenko, T. V., Mikisha, A. M., Smirnov, M. A., "Explosions on the Geostationary Orbit," Advances in Space Research, Vol.19, No.2, 1996, pp.313–319. doi: 10.1016/S0273-1177(97)00014-8
  8. Kiladze, R. I., Sochilina, A. S., Grigoriev, K. V., Vershkov, A. N., "On Investigation of Long-term Orbital Evolution of Geostationary Satellites," Proceedings of the 12th International Symposium on Spaceflight Dynamics, ESA SP-403, Darmstadt, Germany, 1997, pp.53-57.
  9. Johnson, N., Krisko, P., Liou, J.C. et al. Nasa's new breakup model of evolve 4.0. Adv. Space Res. 28 (9), 1377-1384, 2001.
  10. Hanada, T., Yasaka, T. Orbital evolution of cloud particles from explosions of geosynchronous objects. J. Spacecraft 42 (6), 1070–1076, 2005.
  11. Uetsuhara, M., Hanada, T., Yanagisawa, T., et al. Strategy to search fragments from breakups in GEO, Adv. Space Res. 49 (7), 1151-1159, 2012.
  12. Okumura, S., Yanagisawa, T., Nakaya, H., et al. Application of the Time Delay Integration Method: Survey Observations of Geosynchronous Orbit Objects and Short-Term Variability Observations, Publications of the Astronomical Society of Japan (accepted), 2014.

## Publications

### Journal Papers

1. Hanada, T., Uetsuhara, M., Kitazawa, Y., Yanagisawa, T., "Effective Search Strategy Applicable for Breakup Fragments in the Geostationary Region," Journal of Spacecraft and Rockets, Vol.50, No.4, 2013, pp.802-806.
2. Uetsuhara, M., Hanada, T., "Practical Method to Identify Orbital Anomaly as Spacecraft Breakup in the Geostationary Region," Advances in Space Research, Vol.52, No.6, 2013, pp.1072-1077.
3. Hanada, T., "Orbital Debris Modeling and Applications at Kyushu University," Procedia Engineering, Vol.67 (7th Asia-Pacific Conference on Aerospace Technology and Science, 7th APCATS 2013), 2013, pp.404-411.
4. Seto, Y., Hanada, T., Kitazawa, Y., "Characterizing Breakup Fragments for Planning and Observations Using Time Delay Integration," presented at the First Stardust Global Virtual Workshop (SGVW-1) on Asteroids and Space Debris, University of Strathclyde, Glasgow, UK, May 6-9, 2014, also submitted to Advances in Space Research.

### Conference Proceedings

1. Uetsuhara, M., Hanada, T. "Orbital Anomaly Analysis to Detect Breakups in GEO," Paper AAS 14-326 presented at the 24th AAS/AIAA Space Flight Mechanics Meeting, Santa Fe, NM, January 26-30, 2014.
2. Seto, Y., Hanada, T., Kitazawa, Y., "Survey and Origin Identification of Breakup Debris Using Time Delay Integration Method," Paper IAC14,A6,P,74,x25138 presented at the 65th Intl Astronautical Congress, Tronto, Canada, September 29-October 3, 2014.

## APPENDIX A. Time Delay Integration (TDI) method

This section explains the Time Delay Integration (TDI) method and the application of the orbital debris modeling techniques to the TDI method. Figure A.1 schematically explains how the TDI method detects a moving faint object. This method detects a moving faint object by adjusting the rate of charge transfer in the X'-direction (hereinafter, "the TDI scan speed") to the motion vector of the object. The arrows in blue and magenta in Figure A.1 represent the TDI scan speed and the motion vector of orbital object, respectively. The squares in cyan and magenta are the cells on CCD sensor that receive the light of the object and a star at the moment. If the TDI scan speed well matches with the motion vector, the object is imaged as a dot by being

transferred and accumulated the light. In the case of BSGC, the object at 25-40 cm size in GEO can be detected with a 30-seconds exposure [12]. On the other hand, the cell that receives the light of stars is fixed because of sidereal tracking of the telescope. Thus, stars are imaged as strings. Figure A.2 explains an imaging sequence of survey observation. One alignment shot and five images are captured in the image sequence. The stars are fixed on the same position through the image sequence, so that the positions of the detected object in each image can be estimated by only one alignment shot in this method.

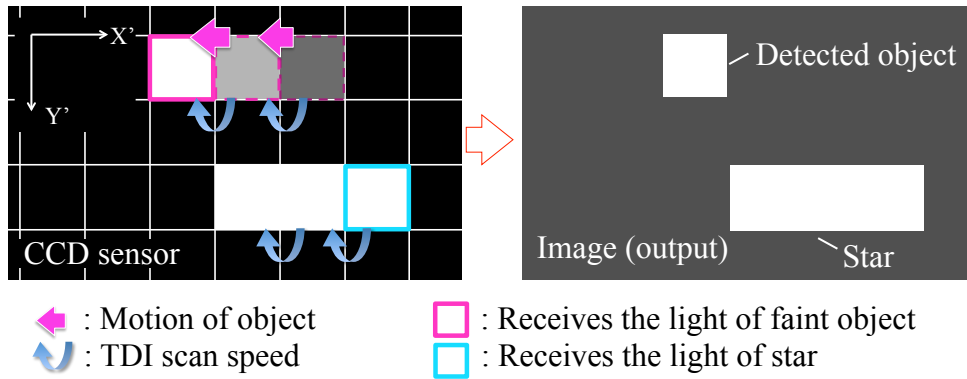


Figure A.1. The detection mechanism of moving faint object by the Time Delay Integration method

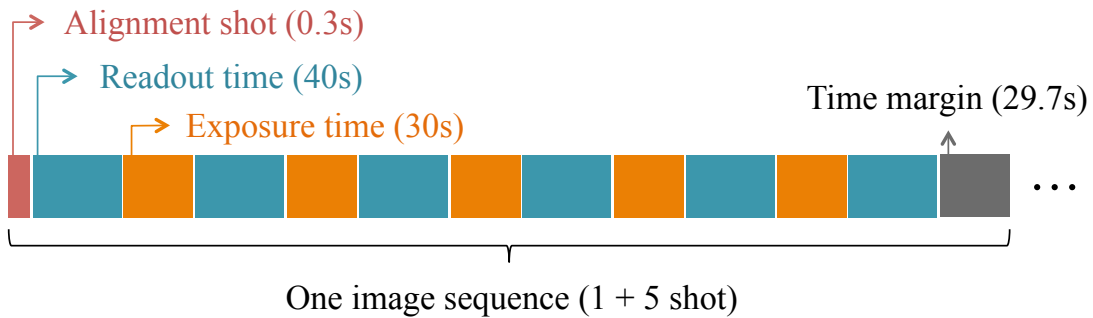


Figure A.2. The imaging sequence

The motion prediction is available for the TDI scan speed determination. Figure A.3 explains how the predicted motion in Figure A.2 can be applied to the TDI method. The CCD sensor needs to be rotated to match the direction of the TDI scan speed vector with the motion vector of the object. X-Y, X'-Y', and R.A.-Dec. represent the Image Coordinate before rotating the CCD sensor, after rotation, and the Geocentric Inertial Coordinate, respectively. In this case, the CCD rotation angle is -6.7 [deg] (+: clockwise), and the TDI scan speed is 15.4[arcsec/sec].

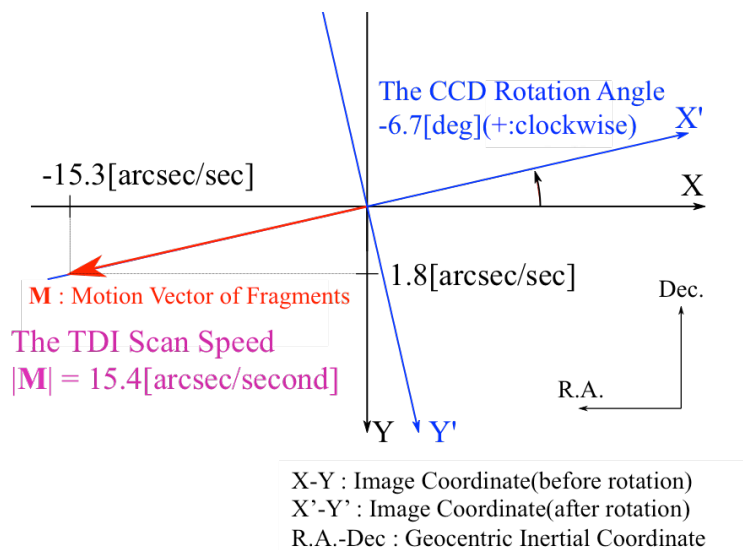


Figure A.3. The TDI scan speed and the CCD rotation angle determination by the predicted motion

## APPENDIX B. Reanalysis of the observation in February 2013

### Observation overview

As the previous granted study reported, search surveys of the possible 1967-066G fragments were conducted from 8 February 2013 to 13 February 2013 at the JAXA Nyukasa Observatory in Nagano Prefecture. Three UCTs, labeled JAXA-d0044, -d0045, and -d0046, respectively, were successfully followed up to determine their orbits precisely. Table 1 summarizes the overview of the observations in February 2013.

Table B.1. The overview of the observation conducted at JNO

Target breakup event	US Titan 3C Transtage (International Designator: 1967-066G)
Observation date	8 <sup>th</sup> , 9 <sup>th</sup> , 13 <sup>th</sup> Feb. 2013 (3 nights)
Observatory	JAXA Nyukasa Observatory, Nagano prefecture, Japan (138°10'18" E, 35°54'05" N, 1870 m altitude)
Telescope	35-cm aperture, 1248 mm focal length, set on a fork-type equatorial mount
CCD sensor	2048 by 2048 pixel, 1.41 by 1.41 deg., 2.2 arc-seconds/pixel

### Reanalysis of origin identification

The previous granted study has proposed the use of inclination vectors ( $i \cos \Omega, i \sin \Omega$ ) to identify the right origins of UCTs. The comparison in inclination vector between the UCTs and 1967-066G at 05:09:09 GMT on 1 February 1994 indicated that JAXA-d0045 and -d0046 could be associated with 1967-066G. However, JAXA-d0044 still had a chance to be associated with 1967-066G if JAXA-d0045 and -d0046 could not be associated with 1967-066G. Finally, the closest positions of JAXA-d0044, -d0045, and -d0046 with 1967-066G were calculated using their orbits at 05:09:09 GMT on 1 February 1994. The resulting closest positions of JAXA-d0044, -d0045, and -d0046 with 1967-066G were 1934.7 km, 1455.2 km, and 2046.6 km, respectively. It can be concluded, therefore, that JAXA-d0044, -d0045, and -d0046 could not be associated with 1967-066G.

The reason why we revisited the observation in February 2013 is to identify the right targets to be observed from Table 1. Therefore, this granted study applies a probabilistic origin identification to identify a possible origin of the three UCTs labeled JAXA-d0044, -d0045, and -d0046, respectively. For the effectiveness of origin identification, possible origins were selected from Table 1 by applying a k-Nearest Neighbor (k-NN) algorithm to motion feature of the three UCTs. Figure B.1 schematically represents the association using the k-NN algorithm. As summarized in Table B.2, JAXA-d0044 was related with two objects of 1977-092A and 1973-040B. JAXA-d0045 and JAXA-d0046 were related with 1975-118C and 1979-087A, respectively.

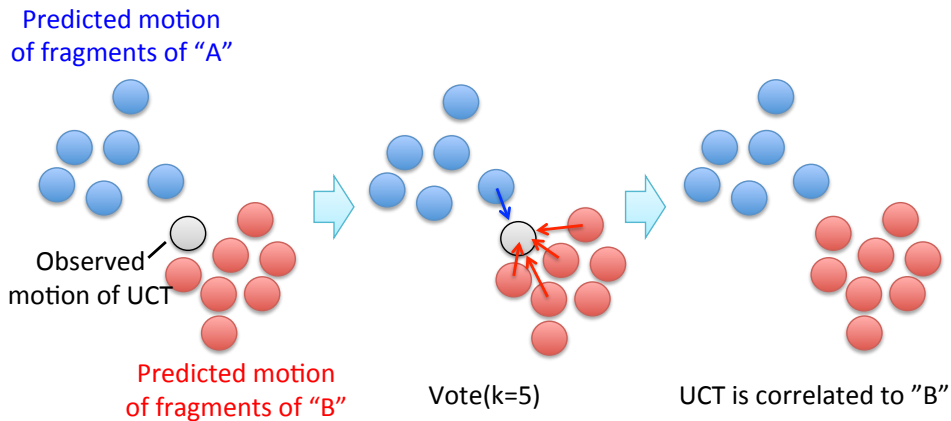


Figure B.1: k-NN algorithm

Table B.2: The results of the k-NN analysis of JAXA-d0044, JAXA-d0045, and JAXA-d0046

Object name	Detection Points	Parent object	# of votes	
			1 <sup>st</sup> night	2 <sup>nd</sup> night
JAXA-d0044	Point A	1977-092A	5	7
		1973-040B	5	3
		1979-087A	1	3
JAXA-d0045	Point B	1979-053C	1	0
		1975-118C	8	7
JAXA-d0046	Point B	1977-092A	1	0
		1979-087A	9	10

To deterministically confirm the relations in Table B.2 we utilized inclination vector and pinch point analyses. As summarized in Table B.3, JAXA-d0046 was associated with 1979-087A. On the other hand, JAXA-d0044 and JAXA-d0045 were not associated with any candidates in Table 1. Figures B.2 and B.3 represent the inclination vector and pinch point analyses of JAXA-d0046 and 1979-087A, respectively. It may be emphasized that the closest position between JAXA-d0046 and 1979-087A was only 16.6 km.

Table B.3: The results of the origin identifications of JAXA-d0044, JAXA-d0045, and JAXA-d0046

Object name	Parent object	Inclination vector	Pinch point	Geocentric distance
JAXA-d0044	1977-092A	Poor	Poor	Poor
	1973-040B	Poor	Poor	Poor
JAXA-d0045	1975-118C	Poor	Poor	Poor
JAXA-d0046	1979-087A	Good	Good	Good

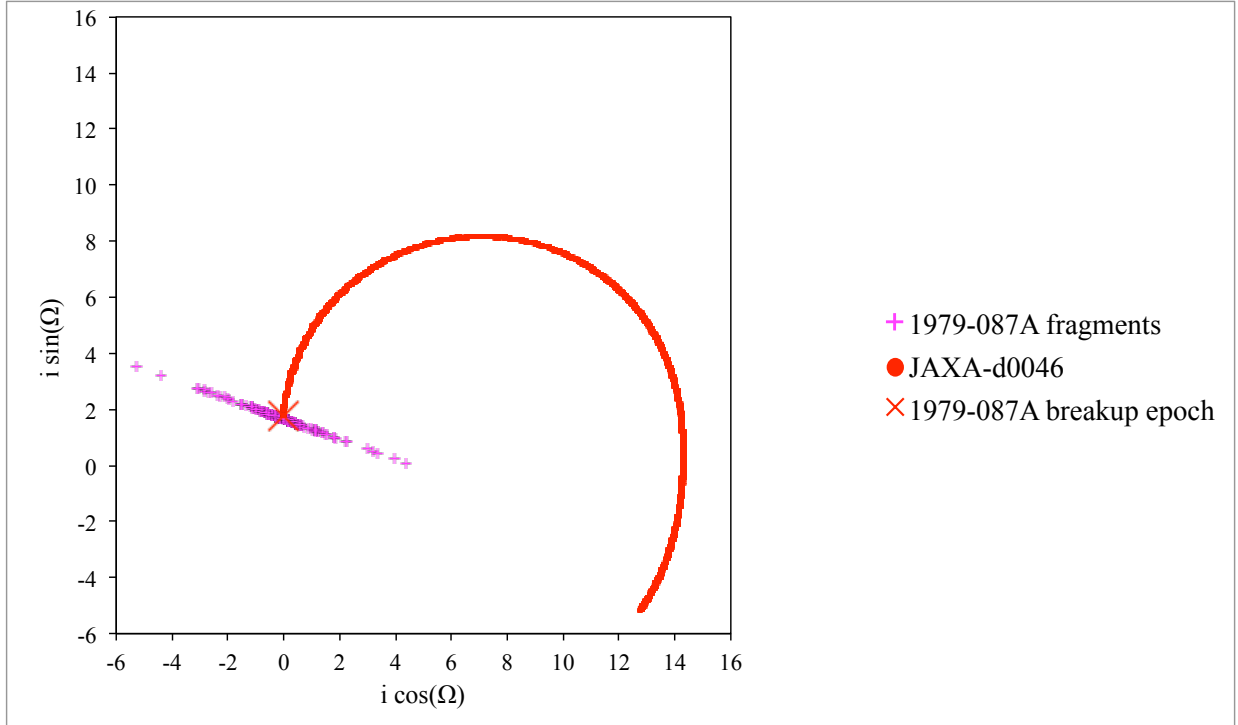


Figure B.2: The inclination vectors ( $i \cos \Omega$ ,  $i \sin \Omega$ ) of 1979-087A and JAXA-d0046 at the breakup epoch of 1979-087A

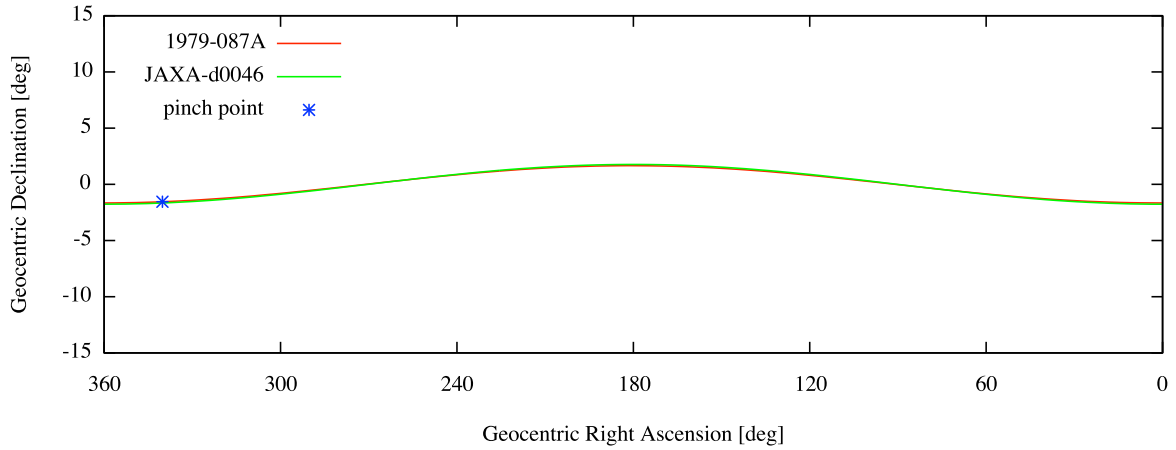


Figure B.3: The pinch point of 1979-087A and the intersection of the orbits of 1979-087A and JAXA-d0046

### APPENDIX C. Review of the proposed strategy

This appendix reviews the proposed search strategy by comparing the predicted motion with 1968-081E catalogued fragments. Twenty-eight objects (1968-081G – 081AK) released from the 1968-081E breakup are now being tracked by Space Surveillance Network (SSN). Figure C.1 shows the motions of the catalogued objects and the predicted motion of the observation point at the epoch x15300 was detected. All the orbits of catalogued fragments except 1968-081X were in the FOV then. Noted that the inclination vector of 1968-081X at the breakup epoch shows different feature from other known fragments. Almost fragments are near the most likely motion, but some fragments, for example, 1968-081V, 081AC and 081AE are a little far from the motion just like x15300. The feature of the motion does not always match with the most likely motion even if the features of the orbit well match with the parent object.

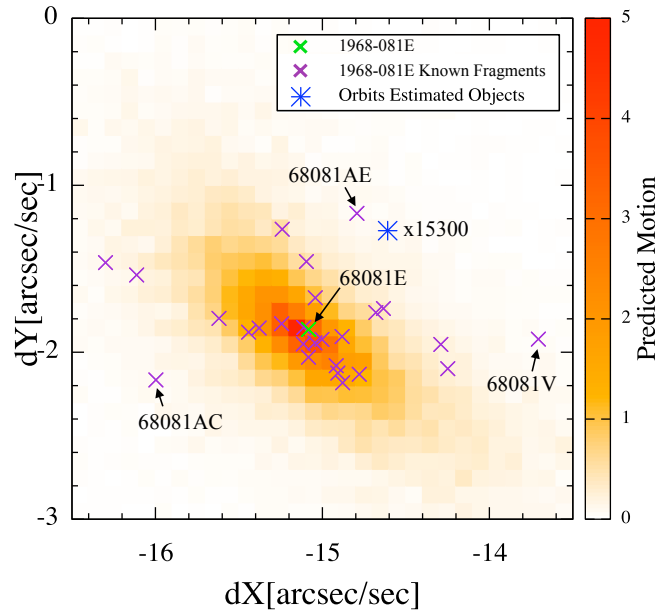


Figure C.1: The motions of 1968-081E catalogued fragments and the predicted motion at the detection epoch of x15300

**APPENDIX D. Other results of origin identification of 1968-081E observation campaign**

This section shows the other results of origin identification of uncorrelated objects detected in 1968-081E observation. Figures D.1 – D.5 represent the results of the analysis of each uncorrelated object. These objects were associated with each parent object at least in terms of the inclination vectors but finally were not correlated with the parents because of the features of radii.

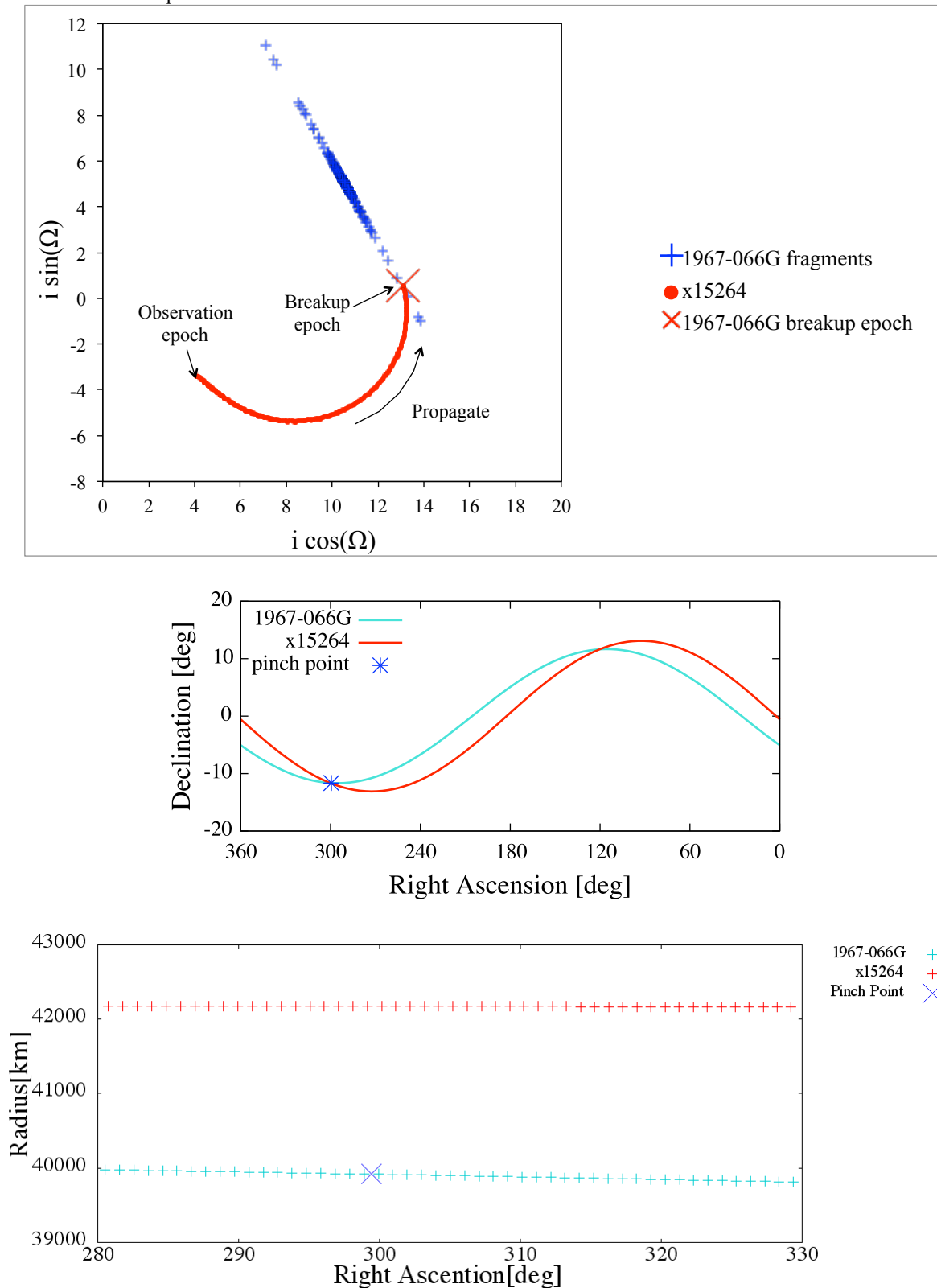


Figure D.1. The origin identification of x15264 with 1967-066G

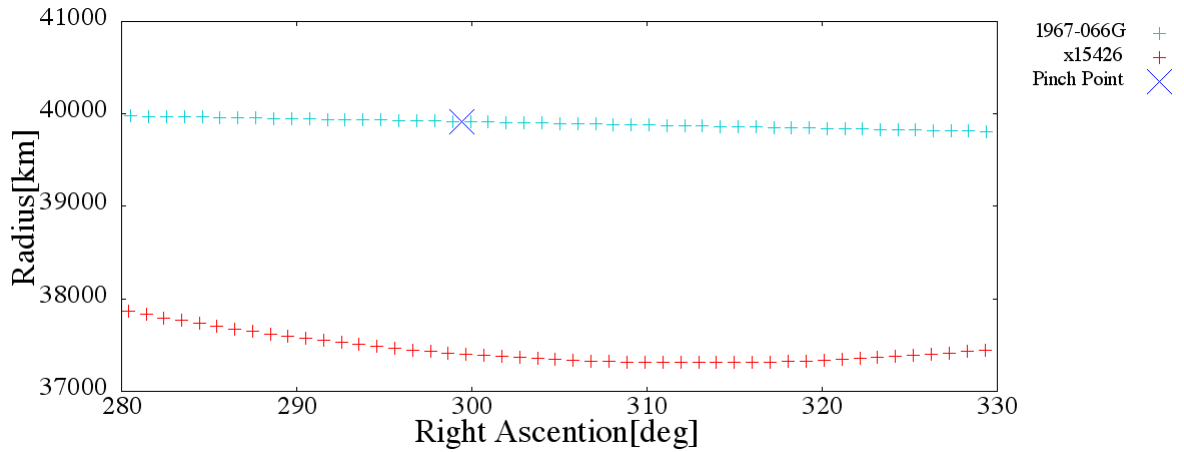
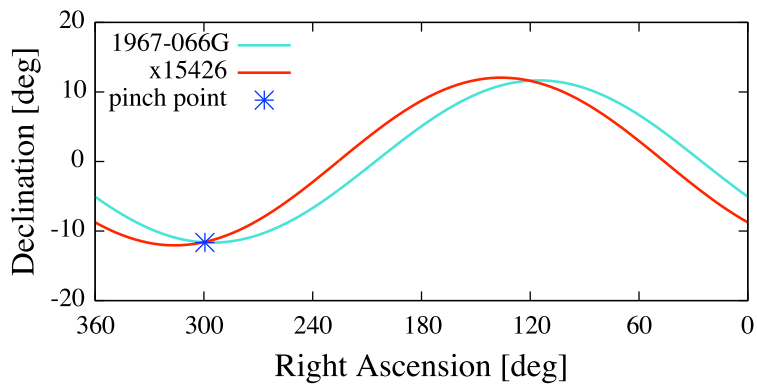
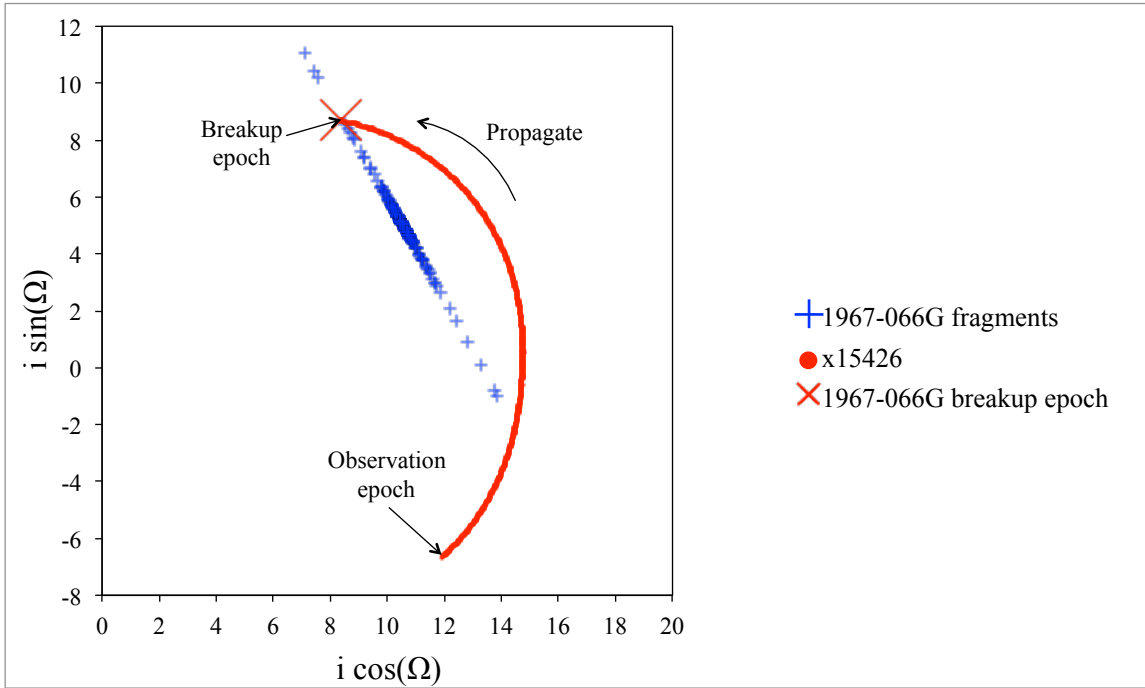


Figure D.2. The origin identification of x15426 with 1967-066G

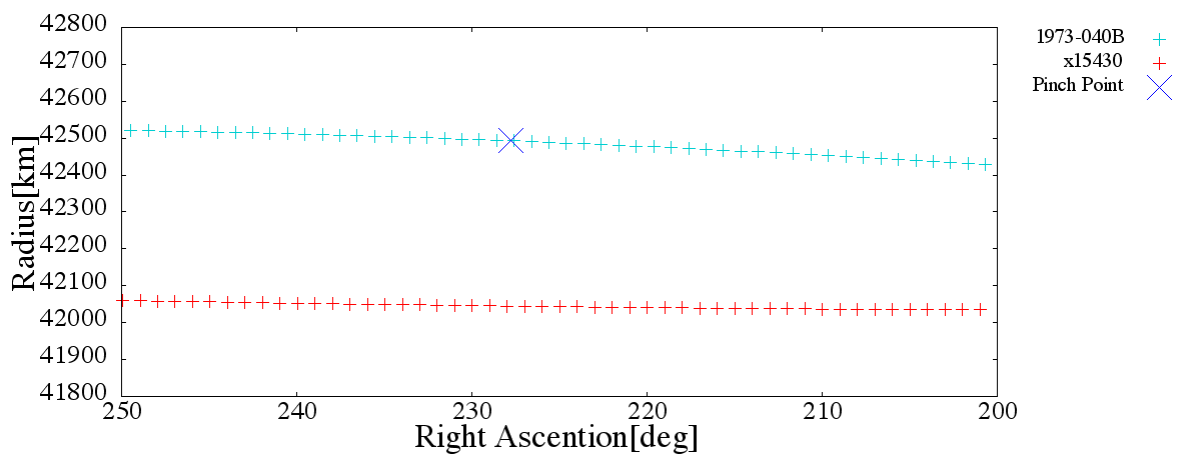
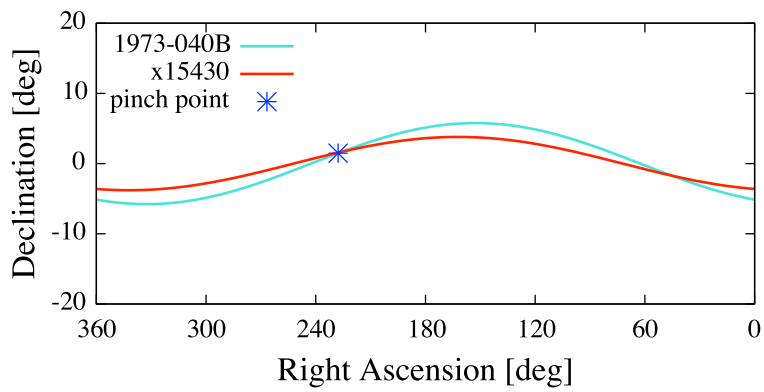
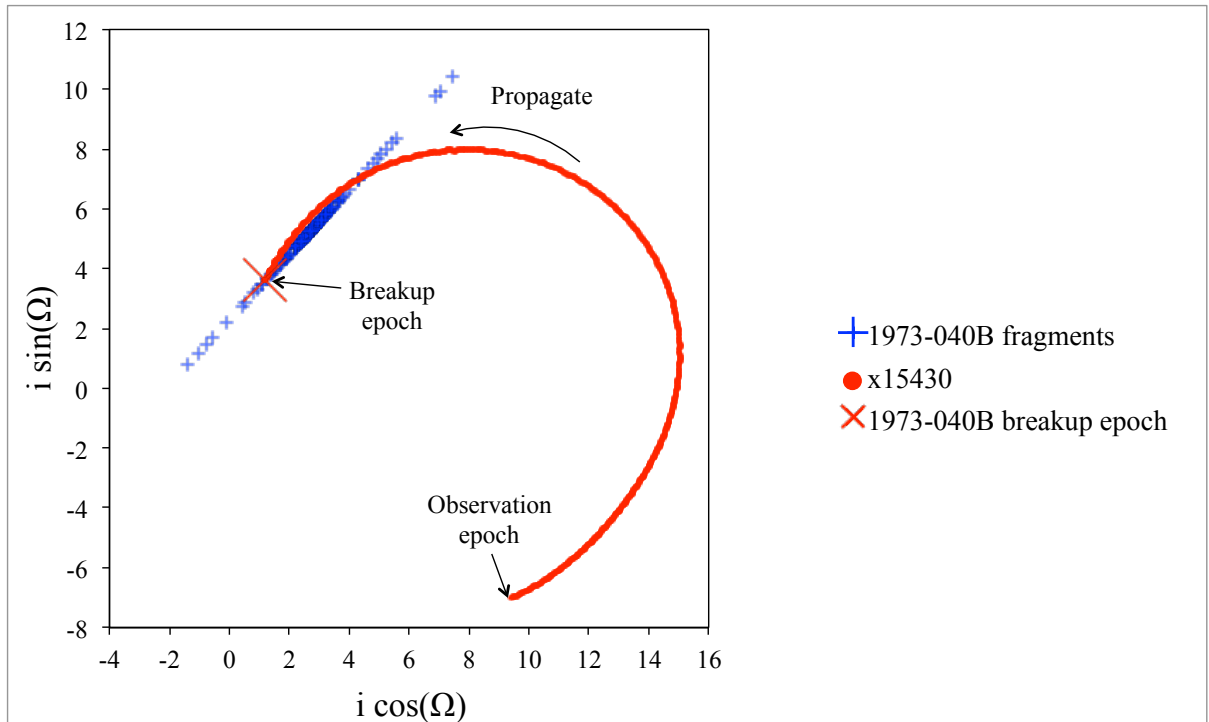


Figure D.3. The origin identification of x15430 with 1973-040B

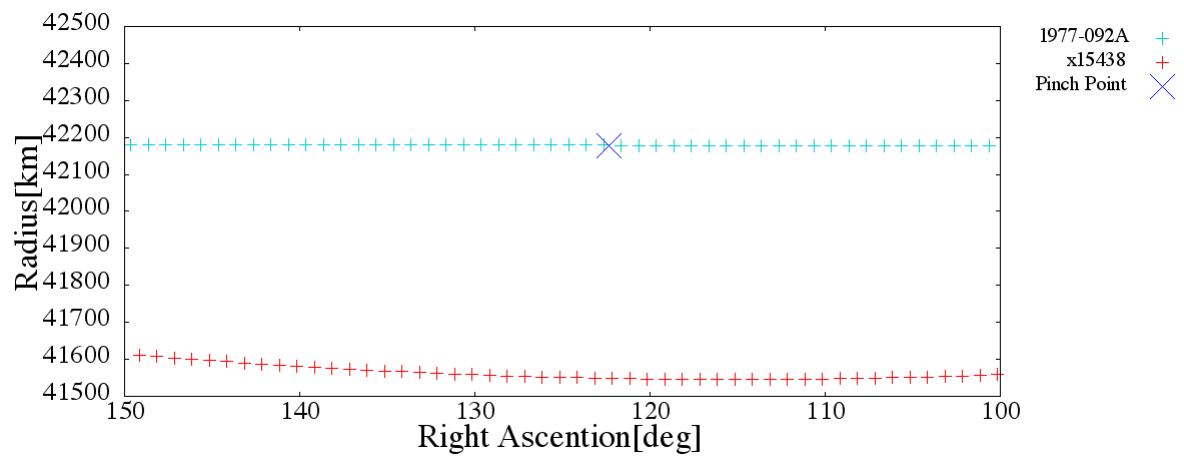
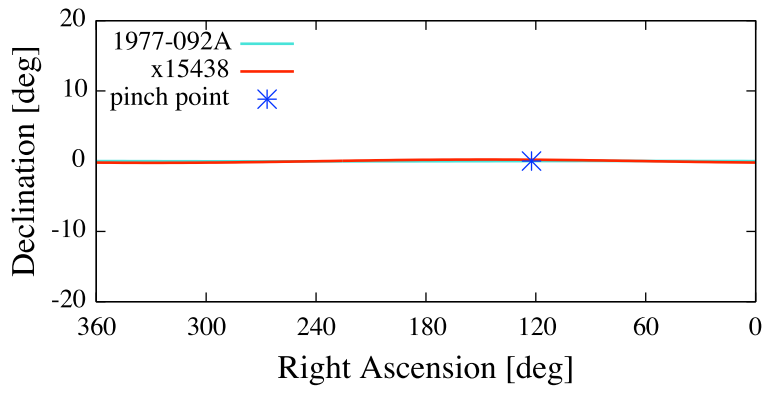
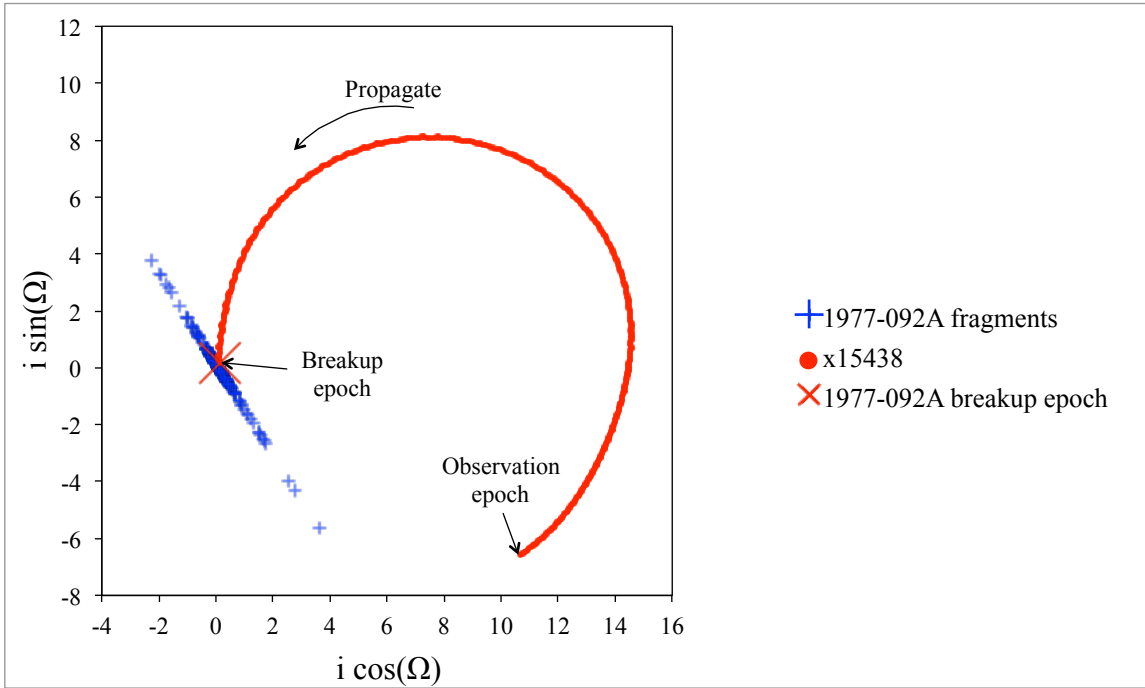


Figure D.4. The origin identification of x15438 with 1977-092A

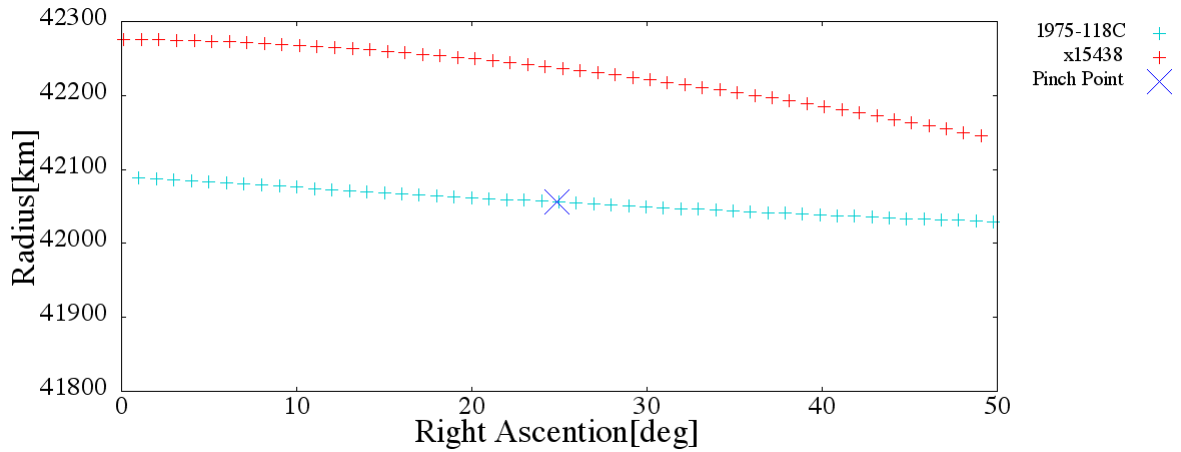
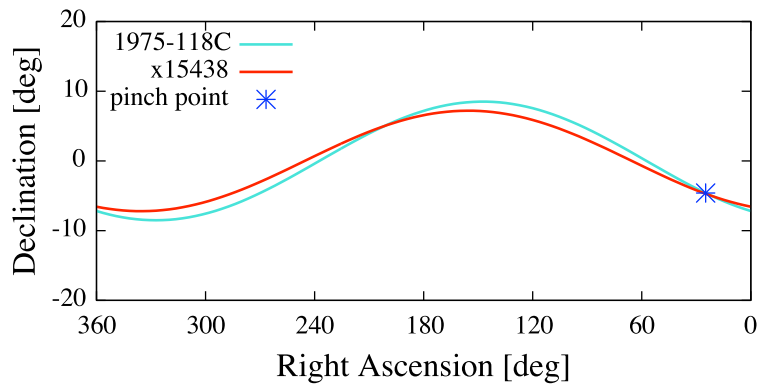
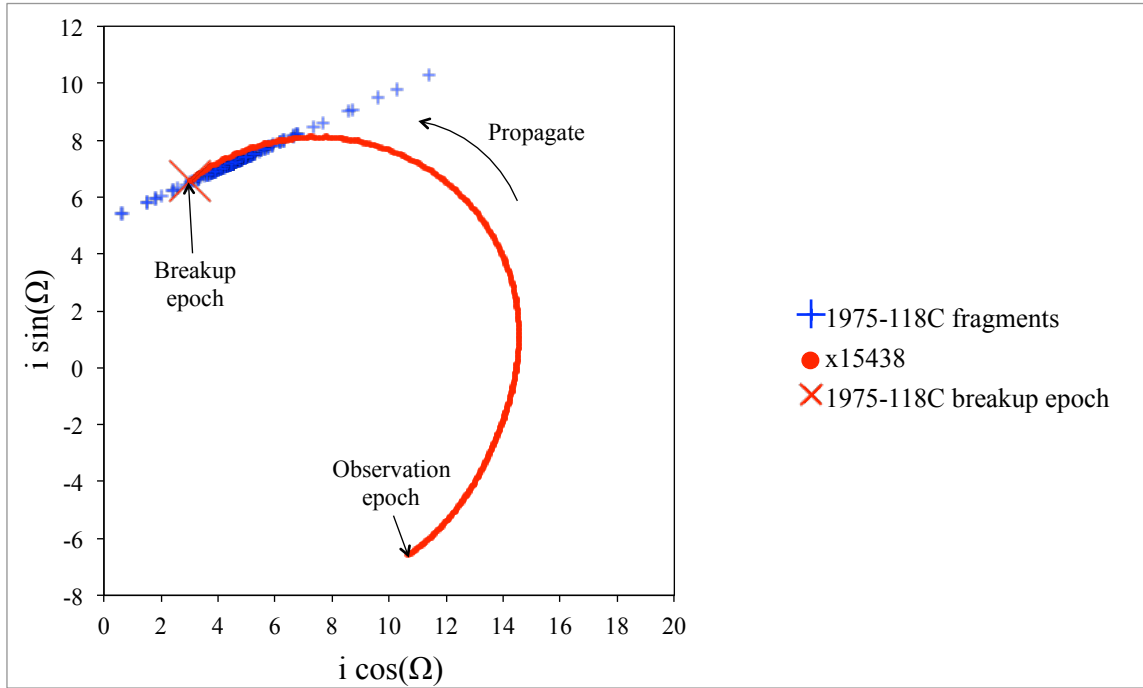


Figure D.5. The origin identification of x15438 with 1975-118C

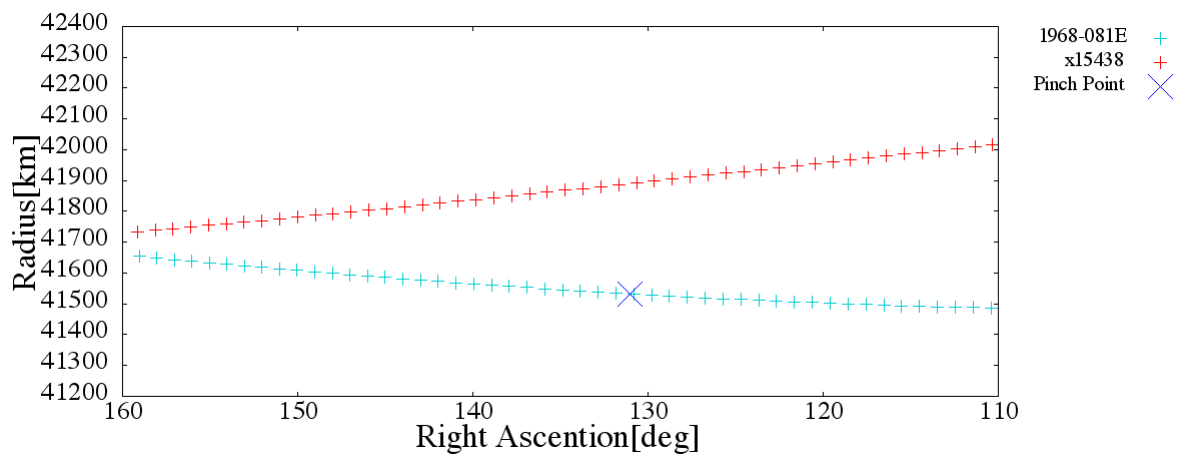
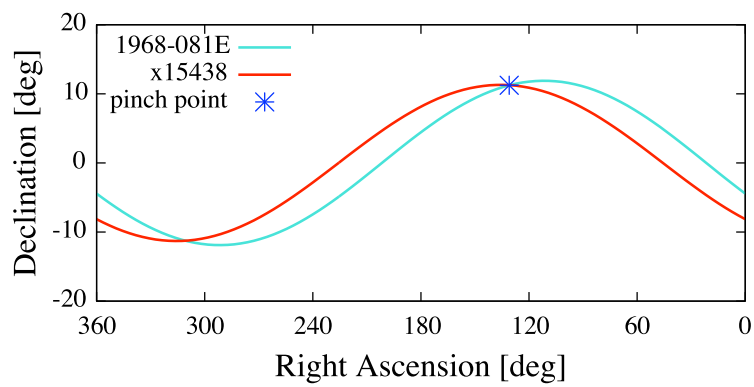
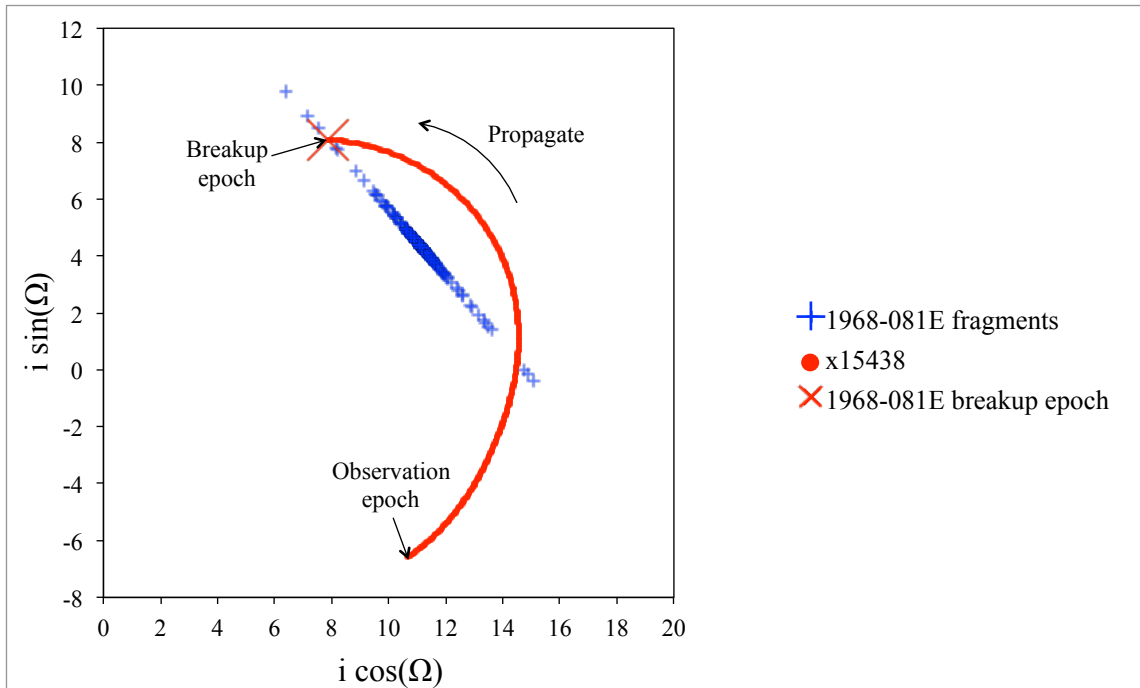


Figure D.6. The origin identification of x15438 with 1968-081E